BBA - Molecular Cell Research 1871 (2024) 119615

Contents lists available at ScienceDirect

BBA - Molecular Cell Research

journal homepage: www.elsevier.com/locate/bbamcr

Research Paper

Two functionally different mitochondrial phosphate carriers support *Drosophila melanogaster* OXPHOS throughout distinct developmental stages

Rosita Curcio [a,1], Luca Frattaruolo [a,1], Federica Marra [a,b,1], Graziano Pesole [b], Angelo Vozza [b], Anna Rita Cappello [a], Marco Fiorillo [a], Graziantonio Lauria [a], Amer Ahmed [b], Giuseppe Fiermonte [b,*], Loredana Capobianco [c,*], Vincenza Dolce [a,*]

[a] Department of Pharmacy, Health and Nutritional Sciences, University of Calabria, 87036 Arcavacata di Rende, Italy
[b] Department of Bioscience, Biotechnology and Environment, University of Bari, 70125 Bari, Italy
[c] Department of Biological and Environmental Sciences and Technologies, University of Salento, 73100 Lecce, Italy

ARTICLE INFO

Keywords:
OXPHOS genes
Mitochondrial phosphate carrier
Drosophila melanogaster
SLC25 solute carrier
CG9090
CG4994

ABSTRACT

The mitochondrial oxidative phosphorylation system (OXPHOS) plays a central role in cellular energy metabolism by producing ATP. In this study, an *in silico* analysis conducted on nuclear somatically expressed *Drosophila melanogaster* OXPHOS genes, revealed shared features including widespread expression, presence of Nuclear Respiratory Gene (NRG) elements, and coordinated developmental-dependent expression, with two distinct peaks of expression during late embryonic and pupal stages. In contrast, OXPHOS paralog genes showed a unique pupal peak and were primarily expressed in adult testes. Furthermore, we conducted an extensive characterization of *D. melanogaster* mitochondrial phosphate carrier (Mpcp), a key player of OXPHOS. In *Drosophila* two genes, CG9090 and CG4994, encode putative Mpcp known as Mpcp1 and Mpcp2. Intriguingly, the expression patterns of Mpcps during development exhibited significant differences from each other and from those of other OXPHOS genes. This suggests that both isoforms contribute to ATP synthesis and are essential for the full organism development, with CG9090 also showing a connection with lifespan and aging processes. Functional complementation assays, swelling experiments carried out in the yeast *mir1*Δ strain and an extensive kinetic characterization of recombinant mature Mpcp2 confirmed that both isoforms transport phosphate. However, Mpcp1 displays a three folds lower activity compared to Mpcp2. Collectively, these findings suggest that mMpcp1 and mMpcp2 operate similarly to mammalian PiC-A and PiC-B, respectively. This provides a basis for exploring functional differences in mammals and gaining new insights into the mechanisms underlying OXPHOS-related diseases associated to deficiencies in human PiC transporters.

1. Introduction

The mitochondrial oxidative phosphorylation system (OXPHOS) is the main mechanism by which cells synthetize ATP, an important source of energy for many biological processes. The OXPHOS includes five multi-enzymatic complexes (complexes I–IV and complex V, also known as ATP synthase) and two mobile electron carriers (Coenzyme Q and cytochrome *c* (Cytc)) [1]. Furthermore, two proteins belonging to the mitochondrial carrier family [2], namely the phosphate carrier (PiC) and the adenine nucleotide transporter (ANT), should be regarded as integral components of the OXPHOS. This is because they transport phosphate and ADP into the matrix, enabling the correct functioning of complex V. In brief, PiC catalyzes the import of inorganic phosphate into mitochondria [3], while ANT catalyzes the exchange of cytoplasmic ADP for intramitochondrial ATP [4].

The deficiency of any component of the OXPHOS is responsible of a diverse and extensive group of human pathologies also known as OXPHOS diseases [5]. These disorders consist of a diverse and extensive group of pathologies, resulting from inborn errors of metabolism. This usually exhibit a broad spectrum of symptoms, varying severity, age of onset, and progression, ultimately leading to significant morbidity and premature mortality [5,6]. These pathologies are due to alterations in the ATP synthesis, resulting in an increased generation of reactive oxygen species (ROS), changes in mitochondrial membrane potential and

* Corresponding authors.
E-mail addresses: giuseppe.fiermonte@uniba.it (G. Fiermonte), loredana.capobianco@unisalento.it (L. Capobianco), vincenza.dolce@unical.it (V. Dolce).
[1] These authors contributed equally to this work.

https://doi.org/10.1016/j.bbamcr.2023.119615
Received 18 August 2023; Received in revised form 18 October 2023; Accepted 19 October 2023
Available online 27 October 2023

calcium homeostasis, as well as alteration of different cellular pathways involving mitochondria, which could also promote cancer development and progression [7–9]. Furthermore, the deficiencies of PiC or ANT lead to a defective oxidative phosphorylation [10–12].

It is evident that mitochondria are the primary targets for treating these diseases and a comprehensive understanding of the physiological processes involving these proteins would significantly enhance the advancement of drug development. [13,14]. In this context, substantial aid might stem from utilizing model organisms. *Drosophila melanogaster* should be considered a valuable one due to the presence of orthologs for approximately 75 % of human disease-associated genes [15]. This peculiarity makes it a frequently utilized organism to study human disease [16–18].

In human, the majority of the OXPHOS subunits are encoded by the nuclear genome (nDNA), whereas merely 13 proteins are encoded by the mitochondrial DNA (mtDNA), some of which constitute the core components of the mitochondrial respiratory chain complexes. Furthermore, nuclear OXPHOS genes and those involved in mitochondrial biogenesis and function are highly conserved from flies to humans and, in *Drosophila* can be easily identified by the presence of a DNA regulatory motif known as Nuclear Respiratory Gene (NRG) consisting of a palindromic 10-bp RTTAYRTAAY motifs [2,19,20]. Taken together, these features support the validity of *D. melanogaster* as a model for mitochondrial disorders and more specifically for the deficiencies of OXPHOS genes [18,21–24]. As mentioned above, the mitochondrial phosphate carrier (PiC) is a critical component of OXPHOS [25]. In mammals, two mutually exclusive isoforms, PiC-A and PiC-B, are encoded by the SLC25A3 gene through the alternative splicing of exons 3A and 3B, which in turn encode the N-*termini* of the mature proteins [26,27]. PiC-A is abundantly expressed in heart, skeletal muscle, and pancreas, while PiC-B is ubiquitously expressed and more active than isoform A [3,28,29]. The occurrence of SLC25A3 deficiency is quite rare in humans. So far, six out of seven homozygous mutations have been found to affect the PiC-A isoform [25,30,31]. Patients with these mutations typically display cardiomyopathy accompanied by skeletal myopathy and elevated blood lactate levels [25,31]. Furthermore, two heterozygous mutations, in both exon 4 and exon 6. have been identified. These mutations, by constraining the required conformational changes for the regular transport function, affect both PiC isoforms function [30].

Two mitochondrial phosphate carrier isoforms have been also identified in *Saccharomyces cerevisiae.* The primary PiC isoform in yeast is Mir1p, which is encoded by the MIR1 gene (YJR077c). Mir1p plays a crucial role in oxidative phosphorylation, as its deletion (*mir1*Δ) makes the yeast strain unable to grow on non-fermentable glycerol [32]. In addition to Mir1p, a second isoform of the phosphate carrier called Pic2p is present in yeast, encoded by the YER053c. The role and localization of this protein is still a matter of debate. On one hand, Hamel and colleagues found this protein to be localized into mitochondria and upregulated at high temperature, suggesting a functional role in specific stress conditions [33]. On the other hand, Takabatake and colleagues reported a vacuolar localization for this protein suggesting that, during evolution, PiC2p may have lost its function and/or mitochondrial targeting, hence retaining only Mir1p as the sole phosphate transporter in yeast mitochondria [34].

In *D. melanogaster*, two genes, CG9090 and CG4994, have been identified as encoding putative mitochondrial phosphate carriers, named Mpcp1 and Mpcp2, respectively [35]. Unlike other characterized mitochondrial carriers in *Drosophila*, where, in the presence of multiple isoforms only one is expressed in somatic tissues while the expression of other isoforms is confined to testis, [2,36–39], both Mpcp1 and Mpcp2 are somatically expressed [35].

The existence of two distinct genes encoding mitochondrial phosphate carriers in *D. melanogaster* can indeed be a valuable starting point for exploring the specific functional differences between the two mammalian isoforms. By studying the expression patterns, functional characteristics, and regulatory mechanisms of the *Drosophila* isoforms (Mpcp1 and Mpcp2), we could potentially gain new insights into the distinct properties and functions of each isoform. This knowledge can subsequently be utilized to elucidate the initiation and mechanisms of OXPHOS diseases caused by deficiencies in the PiC carriers in humans [25]. The *Drosophila* offers a valuable resource for enhancing our understanding of isoform-specific deficiencies in human OXPHOS diseases and could contribute to the development of potential therapeutic strategies.

In this work, the developmental-dependent expression of all OXPHOS genes in *Drosophila* has been investigated through an *in silico* study. The findings unveiled that the OXPHOS genes in *Drosophila* exhibit coordinated expression patterns during development, characterized by two peaks of expression at the late embryonic and pupal stages. Remarkably, the study has emphasized that both *Drosophila* phosphate carriers are classified as OXPHOS genes and hold pivotal roles in the organism's survival across distinct developmental stages. Notably, their developmental-dependent expression diverges both from each other and from that of other OXPHOS genes. Studies carried out in *S. cerevisiae* demonstrated that both *Drosophila* isoforms, as the mammalian PiC, carry an N-terminal pre-sequence which is removed during their import in the yeast mitochondrial membrane. Functional complementation assays and swelling experiments conducted in *S. cerevisiae mir1*Δ strain confirmed the phosphate transport abilities of both isoforms. The phosphate transport activity of both isoforms was further confirmed by reconstituting the recombinant proteins into liposomes where an extensive kinetic characterization of mature Mpcp2 was carried out. Based on our results, it can be concluded that both *Drosophila* Mpcps isoforms operate as mitochondrial phosphate transporters and are involved in the oxidative phosphorylation. Crucially, their functions might differ throughout distinct developmental stages, indicating a stage-specific contribution to the maintenance of energy production.

2. Material and methods

2.1. Plasmids construction of full-length Mpcps and mature Mpcps in E. coli and in S. cerevisiae vectors

Total RNA was extracted from Oregon R adult flies using the RNeasy Mini Kit (Quiagen) and reverse transcribed as previously described [40]. The cDNA corresponding to the mature coding sequences of Mpcps (mMpcps) were amplified by PCR from reversed-transcribed total RNA, cloned into the modified expression vector pET-21b/V5-His, and expressed in *E. coli* as previously described [41]. Forward and reverse primers were synthesized with additional *Nde*I and *Hind*III sites, respectively. In the case of swelling experiments, the mature forms of Mpcps (mMpcp1, and mMpcp2), and Mir1p were cloned into the yeast expression vector pYES2, which had been previously modified by cloning a target sequence coding for a V5 epitope followed by six histidines (pYES2/V5-His), into *Xho*I-*Xba*I sites under the control of the inducible GAL1 promoter (pYES2-GAL1/V5-His). For yeast functional complementation studies, the cDNAs encoding for the full-length and mature Mpcps and Mir1p were cloned into the pYES2-TDH3/V5-His yeast expression vector which permits the expression of proteins under the control of the constitutive TDH3 promoter instead of that of the inducible GAL1 [42]. For all yeast constructs, forward and reverse primers were synthesized with additional *Hind*III and *Xho*I sites, respectively. All plasmids were sequence-verified. The oligonucleotide primers used to generate plasmids are listed in Supplementary Table S1.

2.2. Expression in E. coli, reconstitution into liposomes and transport assays

mMpcp2 protein was overexpressed in the cytosol of *E. coli* BL21-CodonPlus(DE3)-RIL strain (Stratagene) as inclusion bodies [3]. The

inclusion bodies were purified on a sucrose density gradient and washed at 4 °C with TE buffer (10 mM Tris–HCl, 1 mM EDTA, pH 6.5). The recombinant mMpcp2 protein was solubilized by sarkosyl (N-dodecanoyl-*N*-methylglycine sodium salt) and reconstituted into liposomes in the presence of substrates as previously described [43,44].The reconstitution mixture contained solubilized proteins about 0.8/1.5 μg, 1.4 % Triton X-114, 1.4 % egg yolk phospholipids (Fluka) as sonicated liposomes, 20 mM substrate, 20 mM PIPES pH 6.5, and water to a final volume of 700 μl. The reconstitution mixture was mixed and recycled 13 times through a hydrophobic column of Amberlite beads (Fluka) [38]. External substrate was removed on Sephadex G-75. Transport activity was determined as homologous phosphate/phosphate exchange [38]. Transport at 25 °C was started by adding [^{33}P] phosphate (PerkinElmer) to proteoliposomes and terminated by the addition of 80 mM pyridoxal-5′-phosphate (PLP). In controls, the inhibitor was added at the beginning together with the radioactive substrate, according to the "inhibitor-stop" method [3]. All transport measurements were carried out at the same internal and external pH values (pH 6.5). Finally, the external substrate was removed on Sephadex G-75 columns, and the radioactivity into the liposomes was measured [45]. The experimental values were corrected by subtracting control values. The initial transport rate was calculated from the labeled substrate entered into proteoliposomes after 2 min (in the initial linear range of substrate uptake). The ability of the reconstituted mMpcp2 to transport other substrates was also checked.

2.3. Yeast strains, growth conditions and functional complementation of *mir1Δ* yeast strain

BY4742 (wild-type) and YJR077c (*mir1*Δ) yeast strains were provided by the EUROFAN resource center EUROSCARF (Frankfurt, Germany). The genotype of YJR077c is BY4742; MATα; his3Δ1; leu2Δ0; lys2Δ0; ura3Δ0; YJR077c::kanMX4.

The transformation of *mir1*Δ yeast strain with the aforementioned constructs was carried out using the lithium acetate method [42]. BY4742 and the *mir1*Δ yeast strains were also transformed with the empty vectors and used as positive and negative controls, respectively. Transformants were selected on synthetic complete (SC) medium lacking uracil, supplemented with 2 % glucose. Functional complementation was accomplished on liquid YP medium (1 % Bacto yeast extract, 2 % Bacto Peptone, pH 5.0) in the presence of 2 % glucose (YPD) or 3 % glycerol (YPG) as sole carbon sources. Cultures were started from medium log precultures grown in YPD; then, cells were washed, diluted to an optical density of 0.01 at 600 nm and grown in YPD or YPG. Simultaneously, four-fold serial dilutions of washed cells were spotted on YPD or YPG plates and incubated for 72 h at 30 °C.

2.4. Isolation and swelling of yeast mitochondria

All yeast strains, transformed with the various pYES2-GAL1/V5-His constructs and with the empty plasmid, were grown to exponential phase in YPD, galactose (0.4 %) was added 6 h before harvesting. Mitochondria were isolated according to published procedures [46,47]. The rate of mitochondrial swelling was measured by recording the decrease in A_{546} using a Jenway 7315 spectrophotometer, as described before [32]. The swelling assay was initiated by adding 100 μg of yeast mitochondrial protein to a glass cuvette with 1 ml of solution containing 20 mM Tris, 1 mM EDTA, 5 μM rotenone, 0.1 μM antimycin, and various ammonium salts (NH_4Cl (120 mM) or NH_4Pi (120 mM) or NH_4Asp (80 mM), pH 7.4.

2.5. Purification of recombinant mMpcps by Ni^+-nitrilotriacetic acid-agarose affinity column

Mitochondria from yeast strains were prepared as previously described procedures [46,47] and stored at −80 °C until use. Aliquots (6–7 mg of proteins) were thawed and centrifuged at 25,000 ×*g* for 20 min at 4 °C. The pellet was solubilized, at a final concentration of 12–14 mg protein/ml, with a buffer containing 2.5 % Triton X-114 (w/v), 20 mM NaCl, 2 mg/ml cardiolipin, 20 mM Na_2HPO_4, pH 6.5. After 20 min at 0 °C, the mixture was centrifuged at 25,000 ×*g* for 20 min at 4 °C to obtain a clear supernatant referred to as the extract. Next, 600 μl of the extract was chromatographed on Ni^+-nitrilotriacetic acid-agarose affinity column (Quiagen). Unspecifically bound proteins were washed with the solubilization buffer supplemented with increasing concentrations of histidine. The purified proteins were recovered at a histidine concentration of 10 mM. All chromatographic steps were performed at 4 °C. The transport activity of the purified proteins was assayed as described above.

2.6. Other methods

Yeast total proteins were obtained as previously described [48]. Proteins were analyzed by SDS-PAGE and stained with Coomassie Blue dye or transferred to nitrocellulose membranes. The amount of purified Mpcps was estimated by laser densitometry of stained samples using carbonic anhydrase as a protein standard as described before [49,50]. Western blotting was carried out using a rabbit anti-V5 monoclonal antibody or anti-Cor1 and 2 subunits as previously described [51]. The human sequence of the mitochondrial phosphate carrier was used to screen the Flybase database (www.fruitfly.org) using the BlastP program. Expression pattern of OXPOS gene during development were obtained from modENCODE data. Amino acid sequences were aligned using SnapGene® software, (Insightful Science, San Diego, CA, USA) [52,53]. Statistical analysis was performed as previously described [54].

3. Results

3.1. Sequence characteristics and expression of OXPHOS genes during Drosophila development

The *D. melanogaster* complexes I-V subunits (complex I, http://flybase.org/reports/FBgg0000487; complex II, http://flybase.org/reports/FBgg0000485; complex III, http://flybase.org/reports/FBgg0000484; complex IV, http://flybase.org/reports/FBgg0000488; complex V/ATPase, http://flybase.org/reports/FBgg0000491), Cytc, PiC and AAC (http://flybase.org/), were analyzed for the presence or absence of NRG element (Supplementary Table S2) and for their expression levels during organism development (Supplementary Table S3). Since the NRG element is present only in the OXPHOS complexes subunits encoded by the nDNA [20], those encoded by the mtDNA genes were excluded from this analysis.

Remarkably, with very few exceptions, we found that the 74 genes annotated by FlyBase as encoding constituents of the OXPHOS complexes exhibited common features: i) presence of the NRG element (Supplementary Table S2); ii) presence of a human orthologue (Supplementary Table S2); iii) ubiquitous expression (data available on flybase); and iv) a characteristic developmental expression pattern characterized by the presence of two expression-induced peaks. The first peak starts during the late embryogenesis (22–24 h) and persists throughout larval stages L1–L3 (12h). The second peak, more pronounced, initiates during the pupal stage (day 2), reaches its maximum level in the late pupal stage (day 4), and subsequently decreases with age, irrespective of sex (Fig. 1A, B and Supplementary Table S3).

The heatmap reported in Fig. 1A clearly shows the dual-phase gene expression characterizing *D. melanogaster*'s development. In addition, the evident lower expression of the first two complexes of the electron transport chain is in full agreement with the highly conserved stoichiometric ratio between the different OXPHOS complexes ($[1]_{cI}$:$[1–1.5]_{cII}$:$[3]_{cIII}$:$[6–7.5]_{cIV}$:$[3–4]_{cV}$) reported by several groups in different mammalian species [55,56]. In order to graphically highlight the two expression peaks in larval and late pupal stages, we normalized the various developmental expression levels of each subunit to the

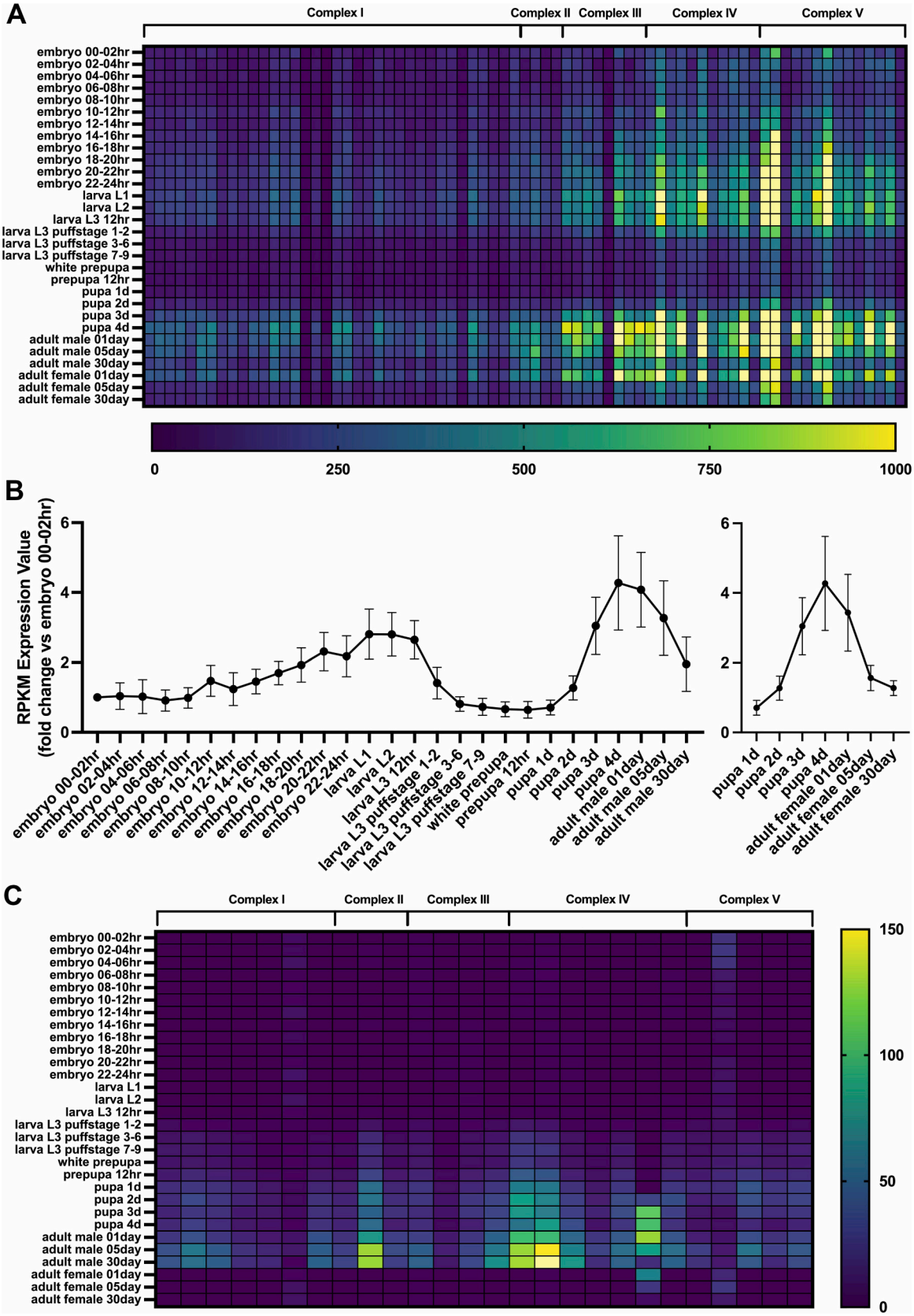

Fig. 1. Expression of OXPHOS genes during *Drosophila* development. (A) Expression profile of OXPHOS genes containing the Nuclear Respiratory Gene (NRG) element throughout development. The expression data was obtained from modENCODE. (B) Postembryonic reinduction (00−02 h) of OXPHOS genes containing the NRG element. The expression data was obtained from modENCODE. (C) Expression profile of OXPHOS genes lacking the NRG element during the development. RPKM (Reads Per Kilobase of transcript per Million mapped reads).

expression of itself during the embryonic stage (0−2h) (Fig. 1B).

The above characteristics were missing in few subunits of OXPHOS complexes classified as somatic genes in FlyBase. Specifically, the NRG element was not found in the complex V subunits CG15458, CG15459, and CG17300. These genes are testis-specific and exhibit a developmental expression pattern identical to that characterizing the paralogous genes (detailed below). This suggests that, similarly to the previously reported CG17300 [57], CG15458 and CG15459 might also represent testis-specific paralogs of the ATP synthase subunits. Furthermore, two complex I genes, containing the NRG element, CG15434 and CG34439, showed sex- and tissue-specific expression [58], respectively. Of note, no human orthologs have been identified for the complex I (CG9034) and complex IV (CG7630) subunits, as well as no temporal expression data were available for the complex III subunit, CG3560.

The 26 genes annotated as paralogs by Flybase share distinctive features: i) absence of the NRG element; ii) expression primarily restricted to the adult testis; and iii) presence of a single expression peak that initiates at the pupal stage (1-day) and increases throughout development, reaching its maximum in adult males at 5 or 30 days depending on the gene considered (Fig. 1C and Supplementary Table S3). We also found a few exceptions: the genes for complex I (CG40472) and complex IV (CG34172) were not expressed in a sex-specific manner. Additionally, CG40472 was expressed ubiquitously.

The study was completed by analyzing the cytochrome *c* and the two mitochondrial carriers essential for ATP synthesis. Cytochrome c in *Drosophila* is encoded by two genes, CG17903 and CG13263, both of which contain the NRG element but differ in their expression during development (CG17903 shows all features of NRG-containing OXPHOS genes, whereas CG13263 is expressed only in testis and follows the typical expression pattern of paralogous genes). In humans, there is a somatically expressed cytochrome *c* gene [59] and a pseudogene [60].

The *Drosophila* expresses two adenine nucleotide translocator isoforms. The first, named sesB or ANT and encoded by the gene CG16944, contains multiple copies of the NRG element (11 NRG sites) and displays all features of NRG-containing OXPHOS genes (Fig. 2 and Supplementary Tables S2 and S3).

(A) Developmental expression profile of genes CG16944 (adenine nucleotide translocator, sesB or ANT), CG9090 and CG4994 (phosphate carrier isoforms, Mpcp1 and Mpcp2, respectively) in male and (B) female. RPKM (Reads Per Kilobase of transcript per Million mapped reads). Expression values were obtained from the modENCODE dataset.

The second, encoded by the gene CG1683, lacks the NRG element, and is annotated in FlyBase as a paralog showing all features of paralogous genes (Supplementary Table S3). A very striking developmental expression pattern has been observed for the genes encoding the phosphate carrier. In *Drosophila*, there are two isoforms, Mpcp1 and Mpcp2, encoded by the genes CG9090 and CG4994, respectively. Both genes contain the NRG element, but the CG9090 gene shows only one expression peak during the pupal stage and is predominantly expressed in the adult organism. The CG4994 gene is ubiquitously expressed and displays its first expression peak during the larval stage. However, the peak expression during the pupal stage is much less prominent compared to that observed in CG9090 and all other OXPHOS genes (Fig. 2 and Supplementary Tables S2 and S3).

3.2. *Mpcp1 and Mpcp2 function as phosphate transporters in S. cerevisiae*

The sequence alignment of human, *Drosophila*, and yeast PiC proteins (Fig. 3) suggests that, similar to higher eukaryotes, *Drosophila* PiCs may have an N-terminal pre-sequence.

To test this hypothesis, two hypothetical mature proteins (mMpcp1 and mMpcp2) were constructed by removing the first 60 and 44 residues from the full-length Mpcp1 and Mpcp2 proteins, respectively.

Firstly, considering that the yeast *MIR1* null mutant does not grow on respiratory carbon sources [32], we examined whether the expression of full-length and putative mature Mpcps could rescue the growth defect of the *mir1*Δ yeast strain. As shown in Fig. 4(A, B), both mature mMpcp1 and mMpcp2 fully restored the growth defect of the *mir1*Δ yeast strain on glycerol-containing media. Interestingly, the full-length form of Mpcp1 did not show any complementation, whereas the full-length form of Mpcp2 partially restored the *mir*1Δ phenotype.

The effective expression of *Drosophila* proteins and their correct localization were verified by Western blotting carried out on whole cell lysate and purified mitochondria. All proteins were detected in the cell lysates (Fig. 4C) as well as in the purified mitochondria (Fig. 4D). Fig. 4D clearly demonstrated that yeast mitochondria processed the N-terminal sequence present in the full-length proteins. Remarkably, the mitochondrial amounts of mature proteins derived from the processed full-length forms of Mpcps were significantly lower than those expressed as putative mature proteins, suggesting that, although yeast was able to process the *Drosophila* full-length forms and import them into mitochondria, this occurred with a limited efficiency. These findings suggest that both Mpcps carry an N-terminal sequence that must be cleaved to become the mature active form of Mpcps. Given that the further experiments were carried out with the mature forms.

Furthermore, we verified whether the *Drosophila* phosphate carrier isoforms catalyzed a proton-assisted phosphate symport as the yeast and mammalian orthologs [3,32]. The anion/H^+ symport can be efficiently assayed through mitochondrial swelling experiments conducted in an isosmotic solution of the target anion ammonium salt [61]. As expected, mitochondria derived from BY4742 swelled in ammonium phosphate

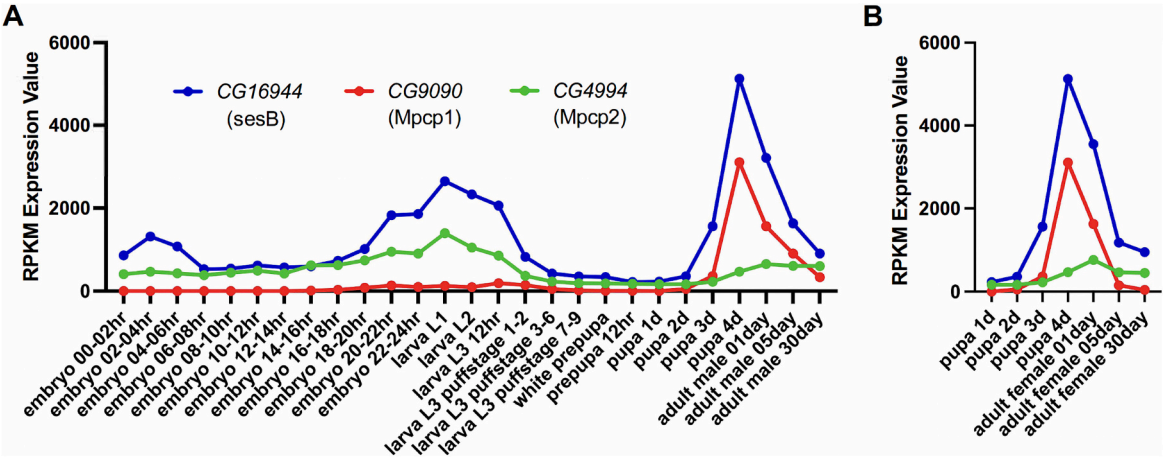

Fig. 2. Expression of mitochondrial carrier protein genes during *Drosophila* development.

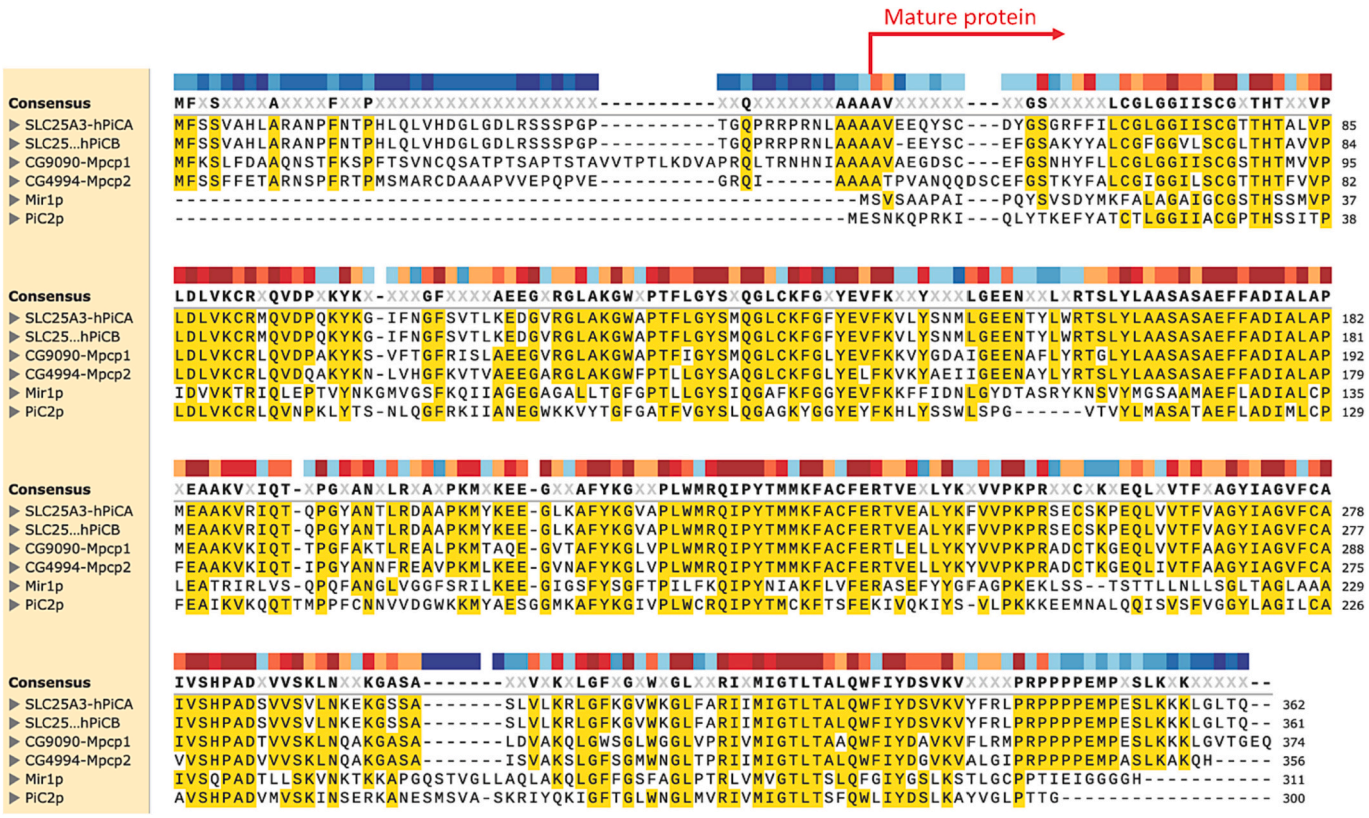

Fig. 3. Alignment of *H. sapiens*, *D. melanogaster*, and *S. cerevisiae* PiC proteins. The arrow indicates the *H. sapiens* mature form.

whereas no swelling was observed with those purified from the *mir1*Δ strain.

Both mitochondria did not swell in ammonium chloride, which was used as a negative control. The integrity of both mitochondria was verified in ammonium aspartate, checking the swelling produced by the proton-assisted aspartate symport catalyzed by the yeast mitochondrial aspartate/glutamate carrier (Agc1p) [61]. The swelling in ammonium phosphate observed in *mir1*Δ strain mitochondria expressing Mir1p, mMpcp1p, and mMpcp2p, indicate that both *Drosophila* proteins catalyze a unidirectional proton-coupled phosphate transport as the endogenous yeast Mir1p (Fig. 4E).

3.3. Expression and functional characterization of recombinant mature Mpcps

Mature Mpcp2 (mMpcp2) was overexpressed at high levels as inclusion bodies (IB) in *E. coli* BL21-CodonPlus(DE3)-RIL. In contrast, no significant expression was obtained with both Mpcp1 and mMpcp1. The IB-purified mMpcp2 gave a single band by SDS-PAGE with an apparent molecular mass of about 36.9 kDa (data not shown).

Approximately 15–20 mg of mMpcp2 per liter of culture were obtained. Recombinant mMpcp2 reconstituted into proteoliposomes was assayed in homo-exchange reactions, using the same substrate inside and outside (20 and 1 mM, respectively). It catalyzed an active [^{33}P]-phosphate/phosphate exchange, no detectable transport activity was found with malate, 2-oxoglutarate, citrate, carnitine, glutamate and aspartate (data not shown). No exchange activity was detected by incorporating into proteoliposomes mMpcp2 that had been previously boiled, or by reconstituting sarcosyl-solubilized material obtained from bacterial cells either lacking the expression vector for mMpcp2 or harvested immediately before the induction of expression (data not shown).

Fig. 5A shows the kinetics of the uptake of 1 mM [^{33}P]phosphate into proteoliposomes reconstituted with mMpcp2 in the presence of 20 mM internal phosphate (exchange) or absence of substrate (unidirectional transport). The exchange and uniport reactions followed first-order kinetics with isotopic equilibrium being approached exponentially. Maximum uptake was approached after 60 min.

The corresponding values at infinite time were 616.31 and 32.61 μmol/mg of protein. The ratio of maximal substrate uptake by exchange and by uniport was 18.89, in agreement with the value of 20 expected from the intraliposomal concentrations at equilibrium (20 and 1 mM for exchange and uniport, respectively). The initial rates of phosphate exchange and uniport, deduced from the respective time courses, were 79.44 and 4.20 μmol/min/mg of protein, respectively. After incubation with 1 mM [^{33}P]phosphate for 60 min, when radioactive uptake had almost approached equilibrium, the addition of 10 mM unlabeled phosphate to proteoliposomes caused an extensive efflux of radiolabeled phosphate from both phosphate-loaded and unloaded proteoliposomes (data not shown). This efflux indicates that [^{33}P]phosphate taken up by exchange or unidirectional transport is released in exchange with externally added substrate. The substrate specificity of mMpcp2 was further investigated by measuring the uptake of [^{33}P]phosphate in proteoliposomes previously loaded with various potential substrates (Fig. 5B). Consistent with previous reports for bovine PiCs expressed in *E. coli* and reconstituted in liposomes [3], high uptake was observed when proteoliposomes contained Pi or arsenate, the mMpcp2 was also able to transport sulfate and thiosulfate, although to a lesser extent. Virtually no exchange was observed with internal malate, fosfomicyn, or ADP (Fig. 5B).

We evaluated the effect of externally added inhibitors on the [^{33}P] phosphate/phosphate exchange reaction catalyzed by mMpcp2 (Fig. 5C). The carrier was almost fully inhibited by pyridoxal 5′-phosphate (PLP), mersalyl, p-chloromercuribenzoate (PCMB), p-chloromercuribenzenesulfonate (PCMBS), and mercuric chloride ($HgCl_2$). A similar inhibitor sensitivity had been previously reported for PiC in intact mitochondria [62] and for the mammalian PiC overexpressed in *E. coli* and reconstituted into liposomes [3,63]. Furthermore, mMpcp2 was strongly inhibited by tannic acid, 2-

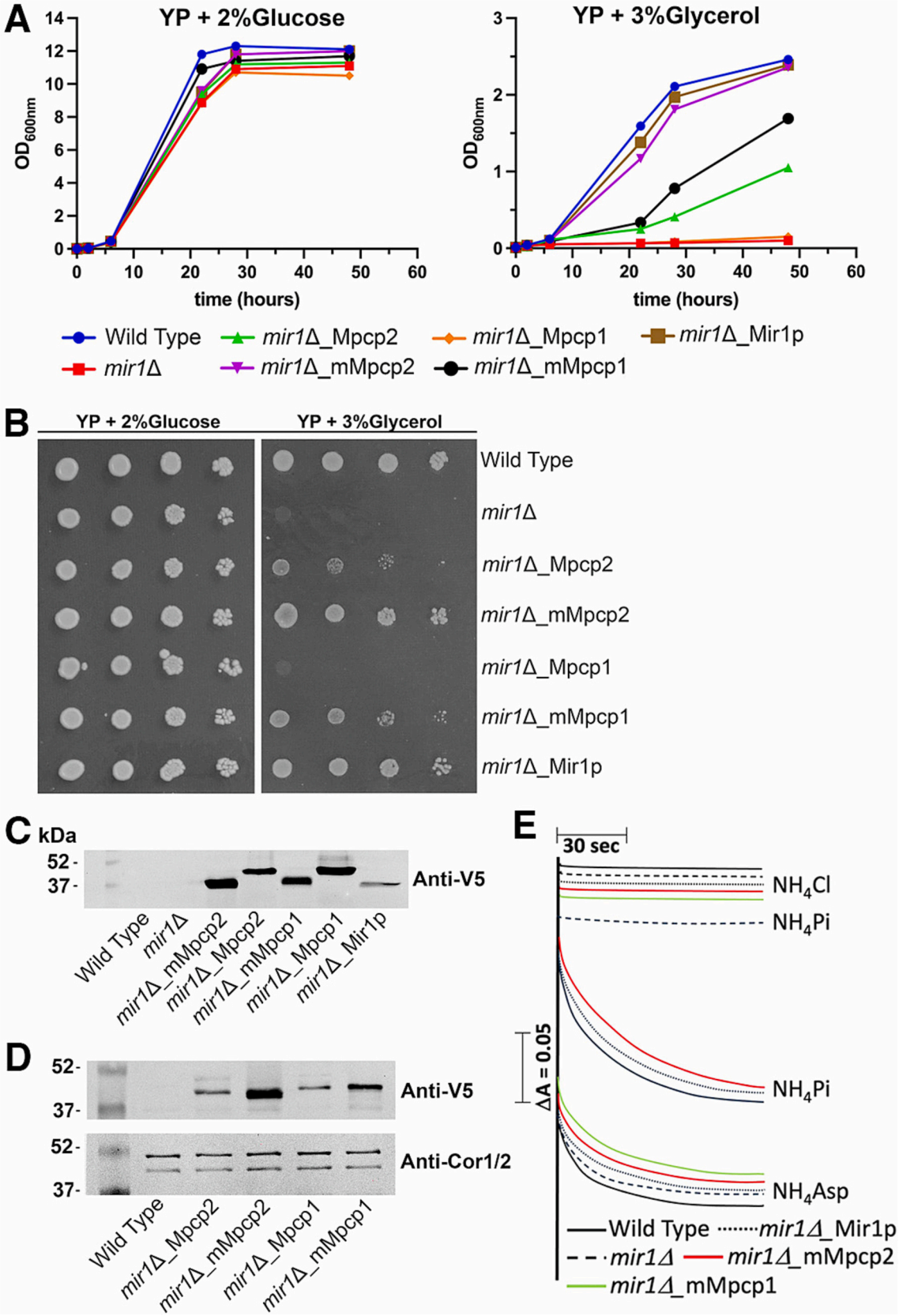

(caption on next page)

Fig. 4. *D. melanogaster* Pic isoforms function as phosphate transporters in yeast cells. (A, B) Growth behavior of *Saccharomyces cerevisiae* BY4742 (wild-type) and *mir1*Δ cells expressing full-length (Mpcps) and mature (mMpcps) *D. melanogaster* PiC isoforms grown on liquid (A) or solid medium (B) containing glucose or glycerol as the sole carbon source. (A) Various transformed yeast strains were inoculated, starting from the same optical density (0.01), in YP medium in the presence of 2 % glucose or 3 % glycerol. The values of optical density at 600 nm refer to cell cultures after the indicated times of growth. (B) Various transformed yeast strains were normalized in water to an optical density of 0.4 at 600 nm. Four serial dilutions of the different cell models were spotted onto YP plates in the presence of 2 % glucose or 3 % glycerol. Plates were grown at 30 °C, and pictures were taken after 3 days. (C) A representative immunoblot of total yeast extract expressing the V5-tagged Mpcps and mMpcps proteins in the *mir1*Δ yeast strain. (D) A representative immunoblot of yeast mitochondria expressing the V5-tagged Mpcps and mMpcps proteins in the *mir1*Δ yeast strain. A yeast anti-Cor1/Cor2 antiserum was used for protein normalization. (E) Swelling of wild-type BY4742, *mir1*Δ and *mir1*Δ expressing mMpcps and Mir1p yeast mitochondria in isosmotic ammonium solutions of various anions. Mitochondria (0.1 mg of protein) were suspended at 25 °C in a solution containing ammonium salts (120 mM NH_4Cl and NH_4Pi; 80 mM ammonium aspartate (NH_4Asp)), 20 mM Tris, pH 7.4, 1 mM EDTA, 0.1 μM antimycin, and 5 μM rotenone in a final volume of 1 ml. Turbidity changes of the mitochondrial suspensions were recorded at 546 nm (see text for more details). A representative experiment from three independent experiments is shown in A, B, and E).

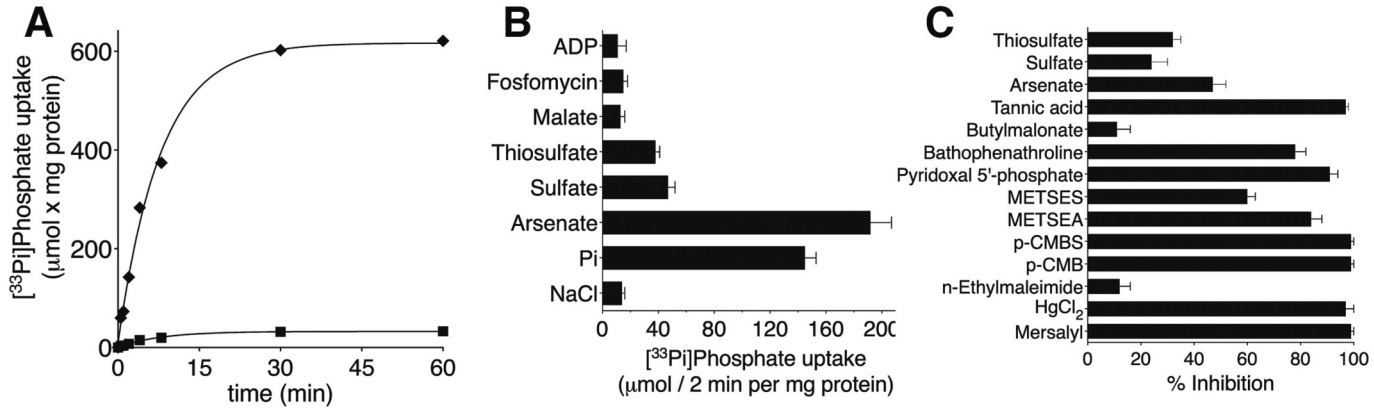

Fig. 5. The bacterial recombinant mMpcp2 catalyzed a phosphate transport. (A) Kinetics of [^{33}P]phosphate uniport and [^{33}P]phosphate/phosphate exchange catalyzed by mMpcp2. Proteoliposomes were reconstituted with mMpcp2. 1 mM [^{33}P]phosphate was added to proteoliposomes containing 20 mM phosphate (exchange, □) or 10 mM NaCl and no substrate (uniport, ■). Similar results were obtained in three independent experiments. (B) Dependence of mMpcp2 transport activity on internal substrate. Proteoliposomes were preloaded internally with various substrates (concentration 20 mM). Transport was started by adding 1 mM [^{33}Pi]phosphate to proteoliposomes reconstituted with mMpcp2 and terminated after 2 min. Data are means ± S.D. of at least three independent experiments. (C) Effect of inhibitors and externally added substrates on the activity of recombinant and reconstituted mMpcp2. Proteoliposomes were loaded with 20 mM phosphate and transport was started by adding 1 mM [^{33}P]phosphate. The incubation time was 2 min. Thiol reagents were added 2 min before the labeled substrate whereas the other inhibitors and external anions were added together with [^{33}P]phosphate. The final concentrations of the inhibitors were 0.1 mM (mersalyl; NEM, n-ethylmaleimide; p-CMB, p-(chloromercuri)benzene acid; p-CMBS, p-(chloromercuri)benzenesulfonic acid), 1 mM (METSEA, 2-aminoethyl methanethiosulfonate hydrobromide; METSES, sodium(2-sulfonatoethyl)-methanethiosulfonate) 20 μM ($HgCl_2$), 10 mM (pyridoxal 5′-phosphate; bathophenanthroline; butymalonate), 0.1 % (tannic acid). Externally-added substrates were used at 5 mM. The control values of uninhibited [^{33}P]phosphate/phosphate exchange (in the absence of inhibitor) were 142 ± 7 μmol/2 min/mg protein. The data represent the means ± S.D. of % inhibition obtained from three independent experiments.

aminoethylmethanethiosulfonate (MTSEA), bathophenanthroline (BAT), and to a lesser extent, by 2-sulfonatoethylmethanethiosulfonate (MTSES). In contrast, butylmalonate and n-ethylmaleimide (NEM), known inhibitors of several mitochondrial carriers [37,61], scarcely affected the transport activity. No significant inhibition was observed with bongkrekic acid and 1,2,3-benzenetricarboxylate [64], which are specific inhibitors of the ADP/ATP and citrate carriers, respectively (data not shown). In addition, the reconstituted [^{33}P]phosphate/phosphate exchange reaction was inhibited by the external addition of arsenate, sulfate and thiosulfate.

The kinetic constants of the recombinant purified mMpcp2 were determined by measuring the initial transport rate at various external [^{33}P]phosphate concentrations, while maintaining a constant saturating internal concentration of phosphate (20 mM). The Km and Vmax values (measured at 25 °C) were 0.9 ± 0.045 mM and 144.096 ± 7.22 μmol/min/mg protein, respectively (five experiments). The activity was calculated by taking into consideration the amount of mMpcp2 recovered from the proteoliposomes after reconstitution.

To prove that mMpcp1 is also a phosphate transporter, both *Drosophila* mMpcp isoforms were expressed in *mir1*Δ yeast strain, purified from mitochondria by a Ni^+-NTA affinity chromatography, reconstituted into liposomes and assayed for their transport function. The data shown in Table 1 highlight that both purified isoforms catalyze a phosphate transport, although mMpcp1 exhibits a lower efficiency compared to mMpcp2.

Table 1
Transport activities of mMpcp1 and mMpcp2 from mitochondria of *mir1*Δ yeast strain. Extract refers to solubilized and reconstituted mitochondria from various yeast strains (*mir1*Δ and *mir1*Δ transformed with Mir1p, mMpcp1 and mMpcp2). Ni^{2+}-NTA eluate refers to mMpcp1 and mMpcp2 purified, by affinity chromatography, from mitochondria of various transformed *mir1*Δ yeast strains. The proteoliposomes were preloaded internally with 20 mM phosphate and the exchange was started by adding 1 mM [^{33}Pi]phosphate and terminated after 1 min. The values are means of three experiments.

Reconstituted proteins	[^{33}Pi]Phosphate uptake (μmol/1 min × mg of protein)
*mir1*Δ extract	0.008 ± 0.0004
*mir1*Δ expressing Mir1p extract	0.035 ± 0.0018
*mir1*Δ expressing mMpcp1 extract	0.013 ± 0.0007
*mir1*Δ expressing mMpcp2 extract	0.049 ± 0.0024
mMpcp1 — Ni^{2+}-NTA eluate	24.9 ± 1.245
mMpcp2 — Ni^{2+}-NTA eluate	78.125 ± 3.906

4. Discussion

Likewise, the somatic genes encoding mitochondrial proteins [20], *Drosophila* nuclear genes encoding somatic subunits of OXPHOS) are characterized by the presence of the NRG element (Table S2). Moreover, we have observed that they exhibit a synchronized developmental-dependent expression pattern that aligns with the energy demands at

different developmental stages. This pattern (Fig. 1A, B and Supplementary Table S3) fully overlaps the gene expression data throughout the entire life cycle of *Drosophila* previously reported [65]. The presence of the first peak, which starts in the late phase of embryogenesis and persists throughout all the subsequent larval stages, can be attributed to the complex metabolic processes that occur during these developmental stages (Fig. 1A, B and Supplementary Table S3). Recent studies indicate that larvae undergo significant metabolic changes compared to other stages [66]. In the larval stage, the organism undergoes a simultaneous increase in body mass and synthesis of triacylglycerol and glycogen, crucial to support pupation and metamorphosis [67,68]. While the high levels of glycolytic enzymes and increased lactate dehydrogenase activity in *Drosophila* suggest that ATP synthesis relies essentially on aerobic glycolysis, it should be noted that an impaired oxidative phosphorylation has a significant impact on organism development [66]. The second peak, significantly more pronounced than the first one, occurs during the late pupal stage (Fig. 1A, B and Supplementary Table S3), is well explained by the structural changes that occur during pupal metamorphosis, rendering this phase highly dependent on oxidative phosphorylation [69]. This remodeling is evident in processes such as programmed cell death in the larval salivary glands [70,71] and in the growth and differentiation of neuroblasts [72]. Furthermore, this second peak well correlates with the U-shaped metabolic curve observed in the measurement of oxygen consumption in *D. melanogaster* pupae during metamorphosis [73], suggesting that starting from the 2-day pupal stage, ATP synthesis becomes strictly dependent on oxidative phosphorylation. We further extended this analysis to the phosphate and the adenine nucleotide carriers, two members of the mitochondrial carrier family [2]. Although they are not usually classified as part of the OXPHOS, it should be emphasized that both transporters provide the intramitochondrial substrates necessary for the correct functioning of the complex V and their loss will affect the whole functioning of OXPHOS. Thus, these two mitochondrial transporters should be included in the OXPHOS genes. Since both carriers are encoded by somatic nuclear genes, we verified whether they exhibited the same features characterizing the OXPHOS genes. As expected, the adenine nucleotide carrier isoform expressed somatically, which is encoded by the CG16944 gene, exhibits all the distinctive features observed in other somatically expressed OXPHOS genes. On the other hand, the isoform testis-specific, encoded by the CG1683 gene, adheres to the rules governing its paralogous genes.

A more complex analysis was required for the mitochondrial phosphate carrier since in *Drosophila* are presence two genes coding for (Mpcp) isoforms and none of them was reported as a paralog gene. The analysis of the developmental-dependent expression of the two genes encoding Mpcp isoforms (CG9090 and CG4994) yielded results different from those observed for ANT and all the other OXPHOS genes (Figs. 1A, B, and 2). *In silico* tissue distribution analysis revealed that CG9090 is predominantly expressed in the adult organism, while CG4994 is ubiquitously expressed (http://flybase.org/reports/FBgn0034497; http://flybase.org/reports/FBgn0026409). Furthermore, the temporal expression of the two genes differs, as CG9090 shows only a peak of expression in the late pupal stage, whereas CG4994 displays the two characteristic peaks of OXPHOS genes. However, it should be noted that the trend of the second peak in CG4994 is significantly lower than those of CG9090 and the other OXPHOS genes (Figs. 1A, B, and 2). These findings strongly indicate that both isoforms are essential to meet the ATP synthesis requirements necessary for the complete development of the organism and that not all genes presenting the NRG element exhibit the two developmental-dependent expression peaks. This conclusion is further supported by the developmental lethality observed when the two genes are individually lost in *Drosophila* (phenotype data from flybase.org). Moreover, the observed reduction in CG9090 mRNA levels during the aging process, particularly in female flies (Fig. 2B), along with literature data, suggest that the expression of CG9090, unlike that of CG4994, is associated with the lifespan and aging of the organism (Fig. 2B). Microarray data show a down-regulation of CG9090 in older flies regardless of sex or genotype [74]. CG9090 is down-regulated in mated females crossed with wild-type males [75], a phenomenon well known to be responsible for life shortening in *Drosophila* females [76]. Moreover, similar to other OXPHOS genes, CG9090 is up-regulated in the Lethal-line of a temperature-sensitive conditional lethal *D. melanogaster* model [77], suggesting that it has a compensatory phosphate transport activity necessary to counteract the suboptimal mitochondrial function in L-line flies.

Since the *in silico* analysis suggested that both genes encode a protein essential for organism development, we verified their phosphate transport function. We initially checked whether *Drosophila* Mpcps carried an N-terminal pre-sequence, similar to mammalian PiCs [26,78,79], as indicated by the alignment of *Drosophila*, human, and yeast phosphate carriers (Fig. 3). The authenticity of the identified pre-sequence was verified by assessing the capability of both the full-length and putative mature isoforms to rescue the growth defect on a non-fermentable carbon source of a yeast strain lacking the endogenous mitochondrial phosphate transporter Mir1p (*mir1*Δ) [32]. The finding that only the mature Mpcp isoforms were detected in mitochondria of the yeast strain transformed with the full-length ORFs (Fig. 4D), indicated that the *Drosophila* proteins possess a processed pre-sequence. Interestingly, although the full-length Mpcps were processed in mature forms they were unable to efficiently complement the growth defect on glycerol of the yeast *mir1*Δ strain (Fig. 4A, B). Conversely, the *mir1*Δ strain transformed with constructs expressing the putative mature isoforms did not show any significant growth delay on glycerol. This apparent discrepancy can be explained by the poor efficiency of the yeast mitochondrial import apparatus on mitochondrial proteins carrying a pre-sequence [32] as also demonstrated by the lower amount of mMpcps found in the mitochondria of yeast strains transformed with the full-length constructs (Fig. 4D). The complementation of the yeast *MIR1* null mutant expressing both mature Mpcps provides indirect evidence of their phosphate transport function (Fig. 4A, B). Swelling experiments carried out on *mir1*Δ mitochondria expressing mMpcps confirmed that both isoforms catalyzed a proton-coupled symport of phosphate similar to the yeast and mammalian orthologs (Fig. 4E). The phosphate transport function of both mMpcps was further verified by reconstituting the His-tagged purified proteins into liposomes. Both proteins catalyzed an efficient Pi/Pi exchange reaction although mMpcp1 was three folds less active than mMpcp2 (Table 1). This different transport activity may explain the lower complementation efficiency of mMpcp1 in the *mir1*Δ strain (Fig. 4A, B).

A complete functional characterization of the bacterial recombinant mMpcp2 revealed that this protein has kinetic properties similar to those found for the bovine phosphate carrier isoform B [3]. In fact, they exhibit comparable Km values (0.9 mM mMpcp2 *versus* 0.78 mM PiC-B) and an overlapping substrate specificity, as they efficiently transport phosphate and arsenate (Fig. 5B). Surprisingly, the *Drosophila* protein is also able to catalyze the transport of sulfate and thiosulfate, albeit with lower efficiency (Fig. 5B). Although the results regarding the function of Mpcps need to be validated directly in *Drosophila*, based on data acquired from *in silico*, *in vitro*, and *in vivo* experiments, it is apparent that mMpcp1and mMpcp2 may function as the *Drosophila* counterparts of the mammalian PiC-A and PiC-B isoforms, respectively.

In fact, similarly to PiC-A and PiC-B, mMpcp1 exhibits a lower activity compared to mMpcp2 and is expressed exclusively in adult stages when the demand for ATP synthesis *via* oxidative phosphorylation increases. It is worth noting that PiC-A is mainly expressed in muscles and heart which rely heavily on oxidative phosphorylation for their energetic needs. In contrast, Mpcp2, like PiC-B, is ubiquitously expressed, display a transport activity higher than that of its counterpart isoform, and has a Km value similar to that of bovine PiC-B [3].

In conclusion, the coexistence of two isoforms (Mpcp1 and Mpcp2) encoded by distinct genes (CG9090 and CG4994, respectively) in *Drosophila*, along with their functional similarity to mammalian

isoforms (PiC-A and PiC-B), provide a promising basis for exploring the specific functional differences of the two human isoforms arisen by an alternative splicing. A further dissecting of the different physiological role of Mpcps may help to better understanding the onset and the pathogenic mechanism of OXPHOS diseases due to the deficiency of the two human PiC isoforms [12,25,31]. The functional analysis of mitochondrial phosphate transporters in fruit flies represents a milestone in understanding the metabolic processes involved during the organism development. Our study further supports the suitability of *D. melanogaster* as an effective model organism for delving into genetics and developmental biology. However, in order to gain a deeper understanding of how the complex transcriptional and expression patterns of OXPHOS genes regulate specific metabolic pathways at different developmental stages of the fruit fly, additional research involving gain and loss of function studies is required.

Supplementary data to this article can be found online at https://doi.org/10.1016/j.bbamcr.2023.119615.

Abbreviations

ANT	adenine nucleotide transporter
METSEA	2-aminoethyl methanethiosulfonate hydrobromide
METSES	sodium(2-sulfonatoethyl)-methanethiosulfonate)
MIR1	mitochondrial phosphate carrier (in yeast)
Mpcp	mitochondrial phosphate carrier protein (in *Drosophila*)
NEM	n-ethylmaleimide
NRG	Nuclear Respiratory Gene
OXPHOS	oxidative phosphorylation system
p-CMB	p-(chloromercuri)benzene acid
p-CMBS	p-(chloromercuri)benzenesulfonic acid
PiC	phosphate carrier
PLP	pyridoxal-5′-phosphate

Funding

This work was supported: by the Italian Ministero dell'Istruzione, dell'Università e della Ricerca, MIUR, 2017PAB8EM_002 (G.F.)

CRediT authorship contribution statement

Conceptualization, V.D., L.C. and G.F.; methodology, R.C., L.F., F.M., G.L., and A.V.; formal analysis, R.C., L.F., F.M, M.F., G.L. A.R.C.; and A. A; investigation, R.C., L.F., F.M, M.F., G.L. A.R.C.; and A.A.; data curation, V.D., G.P., L.C., and G.F.; writing—original draft preparation, V.D., L.C. L.F., F.M. and G.F.; writing—review and editing, V.D., L.C. G.P., and G.F.; supervision, V.D., L.C. and G.F.

Declaration of competing interest

The authors declare that they have no known competing financial interests or personal relationships that could have appeared to influence the work reported in this paper.

Data availability

Data will be made available on request.

Acknowledgements

This work is dedicated to the memory of Professor Corrado Caggese of the University of Bari Aldo Moro. The authors are deeply grateful to Professor Caggese for placing at their disposal all of his extensive knowledge related to the search and identification of the Nuclear Respiratory Gene NRG element, as well as for providing them with preliminary data.

References

[1] S. Nesci, F. Trombetti, A. Pagliarani, V. Ventrella, C. Algieri, G. Tioli, G. Lenaz, Molecular and supramolecular structure of the mitochondrial oxidative phosphorylation system: implications for pathology, Life (Basel) 11 (3) (2021).
[2] R. Curcio, P. Lunetti, V. Zara, A. Ferramosca, F. Marra, G. Fiermonte, A. R. Cappello, F. De Leonardis, L. Capobianco, V. Dolce, *Drosophila melanogaster* mitochondrial carriers: similarities and differences with the human carriers, Int. J. Mol. Sci. 21 (17) (2020).
[3] G. Fiermonte, L. Palmieri, V. Dolce, F.M. Lasorsa, F. Palmieri, M.J. Runswick, J. E. Walker, The sequence, bacterial expression, and functional reconstitution of the rat mitochondrial dicarboxylate transporter cloned via distant homologs in yeast and *Caenorhabditis elegans*, J. Biol. Chem. 273 (38) (1998) 24754–24759.
[4] V. Dolce, P. Scarcia, D. Iacopetta, F. Palmieri, A fourth ADP/ATP carrier isoform in man: identification, bacterial expression, functional characterization and tissue distribution, FEBS Lett. 579 (3) (2005) 633–637.
[5] E. Fernandez-Vizarra, M. Zeviani, Mitochondrial disorders of the OXPHOS system, FEBS Lett. 595 (8) (2021) 1062–1106.
[6] F. Marra, P. Lunetti, R. Curcio, F.M. Lasorsa, L. Capobianco, V. Porcelli, V. Dolce, G. Fiermonte, P. Scarcia, An overview of mitochondrial protein defects in neuromuscular diseases, Biomolecules 11 (11) (2021).
[7] C. Giorgi, F. Baldassari, A. Bononi, M. Bonora, E. De Marchi, S. Marchi, S. Missiroli, S. Patergnani, A. Rimessi, J.M. Suski, M.R. Wieckowski, P. Pinton, Mitochondrial Ca^{2+} and apoptosis, Cell Calcium 52 (1) (2012) 36–43.
[8] K.S. Vikramdeo, S.K. Sudan, A.P. Singh, S. Singh, S. Dasgupta, Mitochondrial respiratory complexes: significance in human mitochondrial disorders and cancers, J. Cell. Physiol. 237 (11) (2022) 4049–4078.
[9] P.S. Brookes, Y. Yoon, J.L. Robotham, M.W. Anders, S.S. Sheu, Calcium, ATP, and ROS: a mitochondrial love-hate triangle, Am. J. Physiol. Cell Physiol. 287 (4) (2004) C817–C833.
[10] F. Fontanesi, L. Palmieri, P. Scarcia, T. Lodi, C. Donnini, A. Limongelli, V. Tiranti, M. Zeviani, I. Ferrero, A.M. Viola, Mutations in AAC2, equivalent to human adPEO-associated ANT1 mutations, lead to defective oxidative phosphorylation in Saccharomyces cerevisiae and affect mitochondrial DNA stability, Hum. Mol. Genet. 13 (9) (2004) 923–934.
[11] E.L. Seifert, A. Gal, M.G. Acoba, Q. Li, L. Anderson-Pullinger, T. Golenar, C. Moffat, N. Sondheimer, S.M. Claypool, G. Hajnoczky, Natural and induced mitochondrial phosphate carrier loss: differential dependence of mitochondrial metabolism and dynamics and cell survival on the extent of depletion, J. Biol. Chem. 291 (50) (2016) 26126–26137.
[12] E.L. Seifert, E. Ligeti, J.A. Mayr, N. Sondheimer, G. Hajnoczky, The mitochondrial phosphate carrier: role in oxidative metabolism, calcium handling and mitochondrial disease, Biochem. Biophys. Res. Commun. 464 (2) (2015) 369–375.
[13] L. Frattaruolo, M. Brindisi, R. Curcio, F. Marra, V. Dolce, A.R. Cappello, Targeting the mitochondrial metabolic network: a promising strategy in cancer treatment, Int. J. Mol. Sci. 21 (17) (2020).
[14] J.A. Smeitink, M. Zeviani, D.M. Turnbull, H.T. Jacobs, Mitochondrial medicine: a metabolic perspective on the pathology of oxidative phosphorylation disorders, Cell Metab. 3 (1) (2006) 9–13.
[15] M.F. Wangler, S. Yamamoto, H.T. Chao, J.E. Posey, M. Westerfield, J. Postlethwait, Members of the Undiagnosed Diseases Network, P. Hieter, K.M. Boycott, P. M. Campeau, H.J. Bellen, Model organisms facilitate rare disease diagnosis and therapeutic research, Genetics 207 (1) (2017) 9–27.
[16] H.S. Gavilan, R.M. Kulikauskas, D.H. Gutmann, R.G. Fehon, In vivo functional analysis of the human NF2 tumor suppressor gene in *Drosophila*, PloS One 9 (3) (2014), e90853.
[17] M.W. Kankel, A. Sen, L. Lu, M. Theodorou, D.N. Dimlich, A. McCampbell, C. E. Henderson, N.A. Shneider, S. Artavanis-Tsakonas, Amyotrophic lateral sclerosis modifiers in *Drosophila* reveal the phospholipase D pathway as a potential therapeutic target, Genetics 215 (3) (2020) 747–766.
[18] S. Vartiainen, S. Chen, J. George, T. Tuomela, K.R. Luoto, K.M. O'Dell, H.T. Jacobs, Phenotypic rescue of a *Drosophila* model of mitochondrial ANT1 disease, Dis. Model. Mech. 7 (6) (2014) 635–648.
[19] D. Porcelli, P. Barsanti, G. Pesole, C. Caggese, The nuclear OXPHOS genes in insecta: a common evolutionary origin, a common cis-regulatory motif, a common destiny for gene duplicates, BMC Evol. Biol. 7 (2007) 215.
[20] M. Sardiello, G. Tripoli, A. Romito, C. Minervini, L. Viggiano, C. Caggese, G. Pesole, Energy biogenesis: one key for coordinating two genomes, Trends Genet. 21 (1) (2005) 12–16.
[21] S. Foriel, P. Willems, J. Smeitink, A. Schenck, J. Beyrath, Mitochondrial diseases: *Drosophila melanogaster* as a model to evaluate potential therapeutics, Int. J. Biochem. Cell Biol. 63 (2015) 60–65.
[22] C. Munnik, M.P. Xaba, S.T. Malindisa, B.L. Russell, S.A. Sooklal, *Drosophila melanogaster*: a platform for anticancer drug discovery and personalized therapies, Front. Genet. 13 (2022), 949241.
[23] S.L. Rea, B.H. Graham, E. Nakamaru-Ogiso, A. Kar, M.J. Falk, Bacteria, yeast, worms, and flies: exploiting simple model organisms to investigate human mitochondrial diseases, Dev. Disabil. Res. Rev. 16 (2) (2010) 200–218.
[24] D.J. Fernandez-Ayala, A. Sanz, S. Vartiainen, K.K. Kemppainen, M. Babusiak, E. Mustalahti, R. Costa, T. Tuomela, M. Zeviani, J. Chung, K.M. O'Dell, P. Rustin, H.T. Jacobs, Expression of the *Ciona intestinalis* alternative oxidase (AOX) in *Drosophila* complements defects in mitochondrial oxidative phosphorylation, Cell Metab. 9 (5) (2009) 449–460.
[25] J.A. Mayr, O. Merkel, S.D. Kohlwein, B.R. Gebhardt, H. Bohles, U. Fotschl, J. Koch, M. Jaksch, H. Lochmuller, R. Horvath, P. Freisinger, W. Sperl, Mitochondrial

phosphate-carrier deficiency: a novel disorder of oxidative phosphorylation, Am. J. Hum. Genet. 80 (3) (2007) 478–484.
[26] V. Dolce, G. Fiermonte, A. Messina, F. Palmieri, Nucleotide sequence of a human heart cDNA encoding the mitochondrial phosphate carrier, DNA Seq. 2 (2) (1991) 133–135.
[27] V. Dolce, V. Iacobazzi, F. Palmieri, J.E. Walker, The sequences of human and bovine genes of the phosphate carrier from mitochondria contain evidence of alternatively spliced forms, J. Biol. Chem. 269 (14) (1994) 10451–10460.
[28] V. Dolce, G. Fiermonte, F. Palmieri, Tissue-specific expression of the two isoforms of the mitochondrial phosphate carrier in bovine tissues, FEBS Lett. 399 (1–2) (1996) 95–98.
[29] M. Huizing, W. Ruitenbeek, L.P. van den Heuvel, V. Dolce, V. Iacobazzi, J. A. Smeitink, F. Palmieri, J.M. Trijbels, Human mitochondrial transmembrane metabolite carriers: tissue distribution and its implication for mitochondrial disorders, J. Bioenerg. Biomembr. 30 (3) (1998) 277–284.
[30] E.J. Bhoj, M. Li, R. Ahrens-Nicklas, L.C. Pyle, J. Wang, V.W. Zhang, C. Clarke, L. J. Wong, N. Sondheimer, C. Ficicioglu, M. Yudkoff, Pathologic variants of the mitochondrial phosphate carrier SLC25A3: two new patients and expansion of the cardiomyopathy/skeletal myopathy phenotype with and without lactic acidosis, JIMD Rep. 19 (2015) 59–66.
[31] J.A. Mayr, F.A. Zimmermann, R. Horvath, H.C. Schneider, B. Schoser, E. Holinski-Feder, B. Czermin, P. Freisinger, W. Sperl, Deficiency of the mitochondrial phosphate carrier presenting as myopathy and cardiomyopathy in a family with three affected children, Neuromuscul. Disord. 21 (11) (2011) 803–808.
[32] V. Zara, K. Dietmeier, A. Palmisano, A. Vozza, J. Rassow, F. Palmieri, N. Pfanner, Yeast mitochondria lacking the phosphate carrier/p32 are blocked in phosphate transport but can import preproteins after regeneration of a membrane potential, Mol. Cell. Biol. 16 (11) (1996) 6524–6531.
[33] P. Hamel, Y. Saint-Georges, B. de Pinto, N. Lachacinski, N. Altamura, G. Dujardin, Redundancy in the function of mitochondrial phosphate transport in *Saccharomyces cerevisiae* and *Arabidopsis thaliana*, Mol. Microbiol. 51 (2) (2004) 307–317.
[34] R. Takabatake, A.B. Siddique, H. Kouchi, K. Izui, S. Hata, Characterization of a *Saccharomyces cerevisiae* gene that encodes a mitochondrial phosphate transporter-like protein, J. Biochem. 129 (5) (2001) 827–833.
[35] R. Sugahara, A. Jouraku, T. Nakakura, M. Minaba, T. Yamamoto, Y. Shinohara, H. Miyoshi, T. Shiotsuki, Tissue-specific expression and silencing phenotypes of mitochondrial phosphate carrier paralogues in several insect species, Insect Mol. Biol. 26 (3) (2017) 332–342.
[36] D. Iacopetta, M. Madeo, G. Tasco, C. Carrisi, R. Curcio, E. Martello, R. Casadio, L. Capobianco, V. Dolce, A novel subfamily of mitochondrial dicarboxylate carriers from *Drosophila melanogaster*: biochemical and computational studies, Biochim. Biophys. Acta 1807 (3) (2011) 251–261.
[37] P. Lunetti, A.R. Cappello, R.M. Marsano, C.L. Pierri, C. Carrisi, E. Martello, C. Caggese, V. Dolce, L. Capobianco, Mitochondrial glutamate carriers from *Drosophila melanogaster*: biochemical, evolutionary and modeling studies, Biochim. Biophys. Acta 1827 (10) (2013) 1245–1255.
[38] A. Vozza, F. De Leonardis, E. Paradies, A. De Grassi, C.L. Pierri, G. Parisi, C. M. Marobbio, F.M. Lasorsa, L. Muto, L. Capobianco, V. Dolce, S. Raho, G. Fiermonte, Biochemical characterization of a new mitochondrial transporter of dephosphocoenzyme A in *Drosophila melanogaster*, Biochim. Biophys. Acta 1858 (2) (2017) 137–146.
[39] Y.Q. Zhang, J. Roote, S. Brogna, A.W. Davis, D.A. Barbash, D. Nash, M. Ashburner, Stress sensitive B encodes an adenine nucleotide translocase in *Drosophila melanogaster*, Genetics 153 (2) (1999) 891–903.
[40] C. Carrisi, M. Madeo, P. Morciano, V. Dolce, G. Cenci, A.R. Cappello, G. Mazzeo, D. Iacopetta, L. Capobianco, Identification of the *Drosophila melanogaster* mitochondrial citrate carrier: bacterial expression, reconstitution, functional characterization and developmental distribution, J. Biochem. 144 (3) (2008) 389–392.
[41] D. Iacopetta, C. Carrisi, G. De Filippis, V.M. Calcagnile, A.R. Cappello, A. Chimento, R. Curcio, A. Santoro, A. Vozza, V. Dolce, F. Palmieri, L. Capobianco, The biochemical properties of the mitochondrial thiamine pyrophosphate carrier from *Drosophila melanogaster*, FEBS J. 277 (5) (2010) 1172–1181.
[42] R. Gorgoglione, R. Seccia, A. Ahmed, A. Vozza, L. Capobianco, A. Lodi, F. Marra, E. Paradies, L. Palmieri, V. Coppola, V. Dolce, G. Fiermonte, Generation of a yeast cell model potentially useful to identify the mammalian mitochondrial N-acetylglutamate transporter, Biomolecules 13 (5) (2023).
[43] R. Curcio, L. Muto, C.L. Pierri, A. Montalto, G. Lauria, A. Onofrio, M. Fiorillo, G. Fiermonte, P. Lunetti, A. Vozza, L. Capobianco, A.R. Cappello, V. Dolce, New insights about the structural rearrangements required for substrate translocation in the bovine mitochondrial oxoglutarate carrier, Biochim. Biophys. Acta 1864 (11) (2016) 1473–1480.
[44] C. Carrisi, D. Antonucci, P. Lunetti, D. Migoni, C.R. Girelli, V. Dolce, F.P. Fanizzi, M. Benedetti, L. Capobianco, Transport of platinum bonded nucleotides into proteoliposomes, mediated by *Drosophila melanogaster* thiamine pyrophosphate carrier protein (DmTpc1), J. Inorg. Biochem. 130 (2014) 28–31.
[45] V. Kurauskas, A. Hessel, P. Ma, P. Lunetti, K. Weinhaupl, L. Imbert, B. Brutscher, M. S. King, R. Sounier, V. Dolce, E.R.S. Kunji, L. Capobianco, C. Chipot, F. Dehez, B. Bersch, P. Schanda, How detergent impacts membrane proteins: atomic-level views of mitochondrial carriers in dodecylphosphocholine, J. Phys. Chem. Lett. 9 (5) (2018) 933–938.
[46] M. Madeo, C. Carrisi, D. Iacopetta, L. Capobianco, A.R. Cappello, C. Bucci, F. Palmieri, G. Mazzeo, A. Montalto, V. Dolce, Abundant expression and purification of biologically active mitochondrial citrate carrier in baculovirus-infected insect cells, J. Bioenerg. Biomembr. 41 (3) (2009) 289–297.
[47] Y. Li, A.R. Cappello, L. Muto, E. Martello, M. Madeo, R. Curcio, P. Lunetti, S. Raho, F. Zaffino, L. Frattaruolo, R. Lappano, R. Malivindi, M. Maggiolini, D. Aiello, C. Piazzolla, L. Capobianco, G. Fiermonte, V. Dolce, Functional characterization of the partially purified Sac1p independent adenine nucleotide transport system (ANTS) from yeast endoplasmic reticulum, J. Biochem. 164 (4) (2018) 313–322.
[48] V.V. Kushnirov, Rapid and reliable protein extraction from yeast, Yeast 16 (9) (2000) 857–860.
[49] R. Curcio, D. Aiello, A. Vozza, L. Muto, E. Martello, A.R. Cappello, L. Capobianco, G. Fiermonte, C. Siciliano, A. Napoli, V. Dolce, Cloning, purification, and characterization of the catalytic C-terminal domain of the human 3-hydroxy-3-methyl glutaryl-CoA reductase: an effective, fast, and easy method for testing hypocholesterolemic compounds, Mol. Biotechnol. 62 (2) (2020) 119–131.
[50] S. Avino, P. De Marco, F. Cirillo, M.F. Santolla, E.M. De Francesco, M.G. Perri, D. Rigiracciolo, V. Dolce, A. Belfiore, M. Maggiolini, R. Lappano, A. Vivacqua, Stimulatory actions of IGF-I are mediated by IGF-IR cross-talk with GPER and DDR1 in mesothelioma and lung cancer cells, Oncotarget 7 (33) (2016) 52710–52728.
[51] R. Lappano, C. Rosano, A. Madeo, L. Albanito, P. Plastina, B. Gabriele, L. Forti, L. A. Stivala, D. Iacopetta, V. Dolce, S. Ando, V. Pezzi, M. Maggiolini, Structure-activity relationships of resveratrol and derivatives in breast cancer cells, Mol. Nutr. Food Res. 53 (7) (2009) 845–858.
[52] C. Peronace, R. Tallerico, M. Colosimo, M. Fazio, F. Pasceri, I. Talotta, G. Panduri, L. Pintomalli, R. Oteri, V. Calantoni, M.T. Fiorillo, M.C. Caroleo, R. Curcio, V. Dolce, E. Cione, P. Minchella, The first identification in Italy of SARS-CoV-2 omicron BA.4 harboring KSF141_del: a genomic comparison with omicron sub-variants, Biomedicines 10 (8) (2022).
[53] D. Iacopetta, R. Lappano, A.R. Cappello, M. Madeo, E.M. De Francesco, A. Santoro, R. Curcio, L. Capobianco, V. Pezzi, M. Maggiolini, V. Dolce, SLC37A1 gene expression is up-regulated by epidermal growth factor in breast cancer cells, Breast Cancer Res. Treat. 122 (3) (2010) 755–764.
[54] F. Aiello, B. Armentano, N. Polera, G. Carullo, M.R. Loizzo, M. Bonesi, M. S. Cappello, L. Capobianco, R. Tundis, From vegetable waste to new agents for potential health applications: antioxidant properties and effects of extracts, fractions and pinocembrin from *Glycyrrhiza glabra* L. aerial parts on viability of five human cancer cell lines, J. Agric. Food Chem. 65 (36) (2017) 7944–7954.
[55] G. Benard, B. Faustin, E. Passerieux, A. Galinier, C. Rocher, N. Bellance, J. P. Delage, L. Casteilla, T. Letellier, R. Rossignol, Physiological diversity of mitochondrial oxidative phosphorylation, Am. J. Physiol. Cell Physiol. 291 (6) (2006) C1172–C1182.
[56] H. Schagger, K. Pfeiffer, The ratio of oxidative phosphorylation complexes I–V in bovine heart mitochondria and the composition of respiratory chain supercomplexes, J. Biol. Chem. 276 (41) (2001) 37861–37867.
[57] E.M. Sawyer, E.C. Brunner, Y. Hwang, L.E. Ivey, O. Brown, M. Bannon, D. Akrobetu, K.E. Sheaffer, O. Morgan, C.O. Field, N. Suresh, M.G. Gordon, E. T. Gunnell, L.A. Regruto, C.G. Wood, M.T. Fuller, K.G. Hales, Testis-specific ATP synthase peripheral stalk subunits required for tissue-specific mitochondrial morphogenesis in *Drosophila*, BMC Cell Biol. 18 (1) (2017) 16.
[58] A.A. Agip, I. Chung, A. Sanchez-Martinez, A.J. Whitworth, J. Hirst, Cryo-EM structures of mitochondrial respiratory complex I from *Drosophila melanogaster*, eLife 12 (2023).
[59] M. Tafani, N.O. Karpinich, K.A. Hurster, J.G. Pastorino, T. Schneider, M.A. Russo, J.L. Farber, Cytochrome c release upon Fas receptor activation depends on translocation of full-length bid and the induction of the mitochondrial permeability transition, J. Biol. Chem. 277 (12) (2002) 10073–10082.
[60] Z.D. Zhang, A. Frankish, T. Hunt, J. Harrow, M. Gerstein, Identification and analysis of unitary pseudogenes: historic and contemporary gene losses in humans and other primates, Genome Biol. 11 (3) (2010) R26.
[61] P. Lunetti, R. Gorgoglione, R. Curcio, F. Marra, A. Pignataro, A. Vozza, C.L. Riley, L. Capobianco, L. Palmieri, V. Dolce, G. Fiermonte, *Drosophila melanogaster* uncoupling protein-4A (UCP4A) catalyzes a unidirectional transport of aspartate, Int. J. Mol. Sci. 23 (3) (2022).
[62] J.P. Wehrle, P.L. Pedersen, Phosphate transport processes in eukaryotic cells, J. Membr. Biol. 111 (3) (1989) 199–213.
[63] R.S. Kaplan, R.D. Pratt, P.L. Pedersen, Purification and characterization of the reconstitutively active phosphate transporter from rat liver mitochondria, J. Biol. Chem. 261 (27) (1986) 12767–12773.
[64] V. Dolce, A.R. Cappello, L. Capobianco, Mitochondrial tricarboxylate and dicarboxylate-tricarboxylate carriers: from animals to plants, IUBMB Life 66 (7) (2014) 462–471.
[65] M.N. Arbeitman, E.E. Furlong, F. Imam, E. Johnson, B.H. Null, B.S. Baker, M. A. Krasnow, M.P. Scott, R.W. Davis, K.P. White, Gene expression during the life cycle of *Drosophila melanogaster*, Science 297 (5590) (2002) 2270–2275.
[66] C.M. Gillette, J.M. Tennessen, T. Reis, Balancing energy expenditure and storage with growth and biosynthesis during *Drosophila* development, Dev. Biol. 475 (2021) 234–244.
[67] C. Heier, R.P. Kuhnlein, Triacylglycerol metabolism in *Drosophila melanogaster*, Genetics 210 (4) (2018) 1163–1184.
[68] J. Mattila, V. Hietakangas, Regulation of carbohydrate energy metabolism in *Drosophila melanogaster*, Genetics 207 (4) (2017) 1231–1253.
[69] C. Sood, S.E. Doyle, S.E. Siegrist, Steroid hormones, dietary nutrients, and temporal progression of neurogenesis, Curr. Opin. Insect Sci. 43 (2021) 70–77.
[70] D.M. Duncan, P. Kiefel, I. Duncan, Mutants for *Drosophila* isocitrate dehydrogenase 3b are defective in mitochondrial function and larval cell death, G3 (Bethesda) 7 (3) (2017) 789–799.
[71] L. Wang, G. Lam, C.S. Thummel, Med24 and Mdh2 are required for *Drosophila* larval salivary gland cell death, Dev. Dyn. 239 (3) (2010) 954–964.

[72] C.C.F. Homem, V. Steinmann, T.R. Burkard, A. Jais, H. Esterbauer, J.A. Knoblich, Ecdysone and mediator change energy metabolism to terminate proliferation in *Drosophila* neural stem cells, Cell 158 (4) (2014) 874–888.
[73] A.B. Merkey, C.K. Wong, D.K. Hoshizaki, A.G. Gibbs, Energetics of metamorphosis in *Drosophila melanogaster*, J. Insect Physiol. 57 (10) (2011) 1437–1445.
[74] W. Jin, R.M. Riley, R.D. Wolfinger, K.P. White, G. Passador-Gurgel, G. Gibson, The contributions of sex, genotype and age to transcriptional variance in *Drosophila melanogaster*, Nat. Genet. 29 (4) (2001) 389–395.
[75] L.A. McGraw, G. Gibson, A.G. Clark, M.F. Wolfner, Genes regulated by mating, sperm, or seminal proteins in mated female *Drosophila melanogaster*, Curr. Biol. 14 (16) (2004) 1509–1514.
[76] A. Koliada, K. Gavrilyuk, N. Burdylyuk, O. Strilbytska, K.B. Storey, V. Kuharskii, O. Lushchak, A. Vaiserman, Mating status affects *Drosophila* lifespan, metabolism and antioxidant system, Comp. Biochem. Physiol. A Mol. Integr. Physiol. 246 (2020), 110716.
[77] K.S. Pedersen, M.C. Codrea, C.J. Vermeulen, V. Loeschcke, E. Bendixen, Proteomic characterization of a temperature-sensitive conditional lethal in *Drosophila melanogaster*, Heredity (Edinb.) 104 (2) (2010) 125–134.
[78] R.D. Pratt, G.C. Ferreira, P.L. Pedersen, Mitochondrial phosphate transport. Import of the H^+/Pi symporter and role of the presequence, J. Biol. Chem. 266 (2) (1991) 1276–1280.
[79] M.J. Runswick, S.J. Powell, P. Nyren, J.E. Walker, Sequence of the bovine mitochondrial phosphate carrier protein: structural relationship to ADP/ATP translocase and the brown fat mitochondria uncoupling protein, EMBO J. 6 (5) (1987) 1367–1373.